Theory of x-ray scattering in high pressure electrides

C. Fortmann, S. H. Glenzer, C. Niemann

June 19, 2012

Disclaimer

This document was prepared as an account of work sponsored by an agency of the United States government. Neither the United States government nor Lawrence Livermore National Security, LLC, nor any of their employees makes any warranty, expressed or implied, or assumes any legal liability or responsibility for the accuracy, completeness, or usefulness of any information, apparatus, product, or process disclosed, or represents that its use would not infringe privately owned rights. Reference herein to any specific commercial product, process, or service by trade name, trademark, manufacturer, or otherwise does not necessarily constitute or imply its endorsement, recommendation, or favoring by the United States government or Lawrence Livermore National Security, LLC. The views and opinions of authors expressed herein do not necessarily state or reflect those of the United States government or Lawrence Livermore National Security, LLC, and shall not be used for advertising or product endorsement purposes.

Theory of x-ray scattering in high pressure electrides

C. Fortmann,[1,2] C. Niemann,[1] and S.H. Glenzer[2]

[1]*University of California Los Angeles, Dept. of Physics and Astronomy, Los Angeles CA 90095, USA*
[2]*Lawrence Livermore National Laboratory, PO Box 808, L-493, Livermore CA 94551, USA*
(Dated: June 1, 2012)

We report on a novel theoretical model for the calculation of x-ray scattering from high pressure electrides. By treating interstitial electrons as effective anions forming a sub-lattice within the crystal, we explicitly account for Bragg reflections from the sublattice as well as for scattering interferences between the ion lattice and the anion sublattice. The additional reflections and interferences lead to significant modifications of the static structure factor as compared to the pure lattices. Our results are important for accurate calculations of material properties in the high pressure phase and further allow for direct experimental verification of electride phases in matter at ultrahigh pressures through angle-resolved x-ray scattering.

Exploration of the equation of state of matter under extreme conditions of pressure, temperature, and density is one of the most challenging adventures of modern science. This research pushes the limits of our understanding about matter at crucial points in the universe, e.g. closely after the big bang, in planetary and stellar interiors, and galactic nuclei [1]. Matter at high energy density ($\sim 10^5$ J/cm^3 = 1 Mbar = 100 GPa) is produced either by direct deposition of intense x-ray radiation (of the order 10^{16} W/cm^2) in a micrometer size target using free electron lasers [2] or by exerting high pressure (several 100s of GPa) on the target. Short pulse lengths of the order 10 fs make free electron lasers suitable to investigate ultrashort processes [3–6], such as non-thermal melting, electronic excitations and relaxation. High pressure techniques produce near equilibrium states that are sufficiently long-lived to investigate their thermodynamic behavior, e.g. the equation of state. The highest pressures in the laboratory are reached today by dynamical compression through interaction of matter with pulsed power in the form of laser pulses, pinches [7], or explosions. A well known example is the inertial confinement fusion approach to reach conditions similar to the interior of the sun through indirect laser drive [8].

Single shock compression is limited to the principle Hugoniot [9] of the target matter, producing high entropy states. Typical temperatures after compression are in the range of several 1000 K, where most materials that are solid at ambient conditions melt and/or transition to a plasma state. Multiple shock compression allows to reach high density states off the principal Hugoniot, i.e. at lower temperature [10]. In the ideal limit of ramp compression (i.e. infinitely many infinitesimally small shocks), the compression becomes isentropic producing superdense states of matter below melting temperature.

High density, low temperature solid phases have recently been investigated using modern ab-initio computer simulation techniques, e.g. density functional theory (DFT) combined with sophisticated structure finding tools [11]. In particular, the structure of simple metals under high pressure (several 10 to several 100 GPa) has received a lot of attention, e.g. sodium [12] potassium [13]), magnesium, [14]) and Al [15]. Surprisingly, these studies showed that valence electrons, instead of becoming increasingly delocalized and Fermi degenerate, as one might naively expect, pair and localize in interstitial cages formed by the still persisting ion lattice [16, 17]. This phenomenon is explained in terms of Coulomb repulsion between valence and core electrons and orthogonality between these states. It was also found that these systems still exhibit metalic or semimetalic conductivity, which is related to the relatively high kinetic energy of electrons within the interstitial cages and interaction effects between the Brillouin zone boundary and the Fermi edge [15, 18].

The existence of such "electride" states of matter was known previously only from certain complex organic and inorganic compounds, see e.g. [19]. Initially, electrides seemed to be of limited practical interest until the first thermally and chemically stable single-crystal electride substance was discovered [20]. Being an optically transparent conductor with unusual magnetic properties, potential applications for electrides include optoelectronic devices, thermoionic power generation, and cooling devices [21].

A direct observation of the electride character of high pressure, low temperature solids is still missing. In this paper, we demonstrate that angle-resolved X-Ray Thomson Scattering (XRTS) is uniquely suited to a) proof the existence of high pressure electride phases, and b) to discriminate between various predicted high pressure electride phases, separated by a structural phase transition. We develop a model for the structure factor $S(\vec{k})$ for electrides. The model is applied to calculate the x-ray scattering profile for magnesium (Mg) at several hundred GPa pressure and room temperature. Under these conditions Mg was predicted to undergo a sequence of phase transitions between various electride structures [14]. Between ~ 500 and 756 GPa, fcc is found to be the most stable crys-

tal structure. In the simulations, valence electrons where shown to localize in the interstitial cages, forming a simple cubic (sc) sublattice. Precisely this sublattice leads to unmistakable features in the scattering profile and thus provides a criterion to experimentally demonstrate the existence of the electride phase: A pure fcc lattice (i.e. without localized interstitial electrons) is characterized by systematic absences at the (100) and (110) Bragg reflection. The interstitial electron sublattice is of sc type and hence shows Bragg peaks at these positions. Above 756 GPa, the structure transitions to a simple hexagonal (sh) phase with interstitial electrons between the honeycomb lattices. Here, interference between electride and ion lattices alters the peak intensities of the (100) and (110) reflection significantly.

Angle-resolved high-energy x-ray scattering experiments will directly measure the new structure peaks from electrides. For example, electride experiments in mm-scale magnesium samples can be approached in static high-pressure diamond anvil cell [22] or in dynamic compression experiments on high-power lasers or pinches [23]. The latter approach is principally capable of producing pressures exceeding those required for producing electrides and further allow dynamic probing with laser-produced Mo K-shell radiation from the He$-\alpha$ transition at 18 keV. These laser-produced plasmas sources provide sufficient photons for single shot observations with high photon energy that will be required to penetrate through mid$-Z$ material. In addition, new free electron laser sources will also provide the required x-ray probe capability [2, 3], particularly when using high-harmonics.

During the x-ray scattering process, the incident photon transfers, on average, momentum $\hbar\vec{k}$ with a Compton energy of $\hbar\omega = \hbar^2 k^2/2m_e = \hbar\omega_0 - \hbar\omega_1$ to the electron, where ω_1 is the frequency of the scattered radiation. For ($\hbar\omega \ll \hbar\omega_0$) and for small momentum transfers we have $\vec{k} = 2\vec{k}_0 \sin(\theta/2)$. Thus, the scattering geometry and the probe energy determine the scattering vector $\vec{k}$

$$k = \left|\vec{k}\right| = 4\pi \frac{E_0}{hc} \sin(\theta/2). \tag{1}$$

Equation (1) determines the scale length of the electron density fluctuations measured in the scattering experiment.

Observing the (100) peak with $k_{100} = 30$ nm^{-1} and $E = 18$ keV requires forward scattering at $\theta = 20°$. For a He$-\alpha$ bandwidth of $\Delta E/E = 2 \times 10^{-2}$ and angular resolution of $\Delta\theta/\theta = 0.25$ we find $\Delta k/k \simeq 0.25$ sufficient to isolate the structural features, cf. Fig. 2.

Interstitial electrons act as anions [19] and can be treated as additional centers of the primitive cell. The scattering profile, i.e. the absolute scattered intensity as function of scattering angle, will be dominated by narrow peaks corresponding to Bragg reflections from the lattice planes. We write the x-ray scattering cross section as

$$\frac{d\sigma}{d\Omega} = \sigma_{\text{Th}} S(\vec{k}) , \tag{2}$$

Here $S(\vec{k})$ is the electron structure factor given by the Fourier transform of the electron-electron pair correlation function. It can be written as [24]

$$S(\vec{k}) = e^{-2W(k)} \frac{(2\pi)^3}{n_e} \sum_{\vec{G}\neq 0} |n_{e\vec{G}}|^2 \delta(\vec{k}-\vec{G}) + \left[1 - e^{-2W(k)}\right] . \tag{3}$$

The first term describes coherent (Bragg) scattering from lattice planes characterized by inverse lattice vectors $\vec{G}$. Their amplitude is given by the Fourier component of the electron density

$$n_{e\vec{G}} = \sum_i f_i \exp(-i\vec{G}\cdot\vec{d_i}) . \tag{4}$$

which coherently sums scattering amplitudes from all sites within the lattice basis $\{\vec{d_i}\}$; $f_i(k)$ is ionic form factor. The Debye-Waller factor $\exp(-2W(k))$ accounts for the reduction in intensity due to thermal lattice vibrations. Correspondingly, thermal diffuse (incoherent) scattering is described through the second term in Eq. (3). Within the Debye model for cubic lattices [25],

$$W(k) = \frac{3}{4k_{\text{B}}T_D} \frac{\hbar^2 k^2}{2m_I} \left(1 + 4\left(\frac{T}{T_D}\right)^2 \int_0^{T/T_D} \frac{x\,dx}{e^x - 1}\right). \tag{5}$$

For simplcity, we assume that interstitial electrons adiabatically follow the ion lattice vibrations, hence only one Debye-Waller factor appears to describe the thermal motion for both lattice ions and interstitial sites.

After separating the electron density $n_{e\vec{G}}$ into core electrons centered around lattice ions (I) and interstitial electrons (X) $n_{e\vec{G}} = n_{I\vec{G}} + n_{X\vec{G}}$, we can rewrite Eq. (3) as

$$S(\vec{k}) = e^{-2W(k)}(2\pi)^3 \sum_{\vec{G}\neq 0} \left| f_I(\vec{k}) \sum_{\text{ion sites}} \exp(-i\vec{k}\cdot\vec{d_i}) + f_X(\vec{k}) \sum_{\text{interst.}} \exp(-i\vec{k}\cdot\vec{d_i}) \right|^2 \delta(\vec{k} - \vec{G}) + \left[1 - e^{-2W(k)}\right]$$
$$= e^{-2W(k)}(2\pi)^3 \left\{ |f_I(\vec{k})|^2 S_{ii}(\vec{k}) + |f_X(\vec{k})|^2 S_{xx}(\vec{k}) + 2\text{Re}\left[f_I(\vec{k})f_X^*(\vec{k})\right] S_{xi}(\vec{k}) \right\} + \left[1 - e^{-2W(k)}\right] , \tag{6}$$

$f_I(\vec{k})$ is the core electron form factor, $f_X(\vec{k})$ is the interstitial electron form factor. In the absence of interstitial electrons, $f_X(\vec{k}) = 0$ and one finds the well-known result for coherent scattering from pure ion lattices [24]. Scatter-

ing interferences between lattice ions and electride anions (electrons) are explicitly taken into account via the "mixed" structure factor $S_{xi}(\vec{k})$. It will be shown that this interference term significantly alters the peak amplitudes when compared to the pure ion lattice. Additional peaks appear when the electride sublattice belongs to a different space symmetry group than the ion lattice.

We apply our model to calculate the total electron structure factor $S(\vec{k})$ for magnesium at pressures between 500 GPa and 800 GPa. Lattice structure parameters (space symetry group, dimensions of the unit cell, and coexistence curves) are taken from Ref. [14]. These simulations predict that Mg undergoes a structural phase transition from bcc to fcc at ~ 456 GPa pressure at room temperature [14]. The length of the primitive lattice vectors in the fcc phase is $a = 2.1$ Å. The electron localization function (ELF) [26] assumes maximum values of ~ 0.91 in the eight interstitial spaces of the fcc primitive cell, forming a simple cubic (sc) lattice. The ELF measures the density distribution of electron pairs and is normalized such that ELF≤ 1. Zeros in the ELF mark the spatial extension of the interstitial electron cloud. For simplicity, we approximate the interstitial electron density by a spherically symmetric gaussian distribution although the simulations predict a more cubical shape. The full width at half maximum is taken as $0.5a$.

The total structure factor and the three partial structure factors $|f_I|^2 S_{ii}(k)$, $|f_X|^2 S_{xx}(k)$, and $2\mathrm{Re}\,[f_I f_X^*]S_{xi}(k)$ are shown in Fig. 1. The structures are averaged over all lattice orientations thus representing scattering from a polycrystalline sample. The bottom x-axis shows the wavenumber k in units of the reciprocal lattice spacing $k_0 = 2\pi/a = 30$ nm^{-1}, the top x-axis shows k in units of 1/nm. The lattice peaks are represented by narrow Gaussians. The total structure factor has an offset of $+50$ for better discernability from the partial structure factors. The fcc ion lattice (black line) is characterized by systematic absences at the (100) ($k = k_0 = 30$ nm^{-1}) and (110) ($k = \sqrt{2}k_0 = 42$ nm^{-1}) position. Here, the interstitial sc lattice produces notable signals. The (111) peak ($k = \sqrt{3}k_0 = 52$ nm^{-1}) is slightly amplified with respect to the pure fcc lattice peak (S_{ii}) due to the interference term S_{xi} and to a small extent from electron lattice scattering. Beyond $k = 2k_0 = 60$ nm^{-1}, the interstitial form factor $f_X(k)$ practically vanishes and sc lattice and interference terms are suppressed. The form factors are shown in the inset in Fig. 1.

Fig. 2 shows the total scattering profile for fcc Mg with (red) and without (black) interstitial electrons, taking into account the Debye-Waller factor and the incoherent contribution (shown in the inset). Bragg peaks at (100) and (110) positions in the electride phase are clearly identified.

At ~ 756 GPa, Mg transitions to the simple hexagonal (sh) phase with interstitial electrons between the honeycomb lattices. The lattice dimensions are $a = 0.189$ nm and $c = 0.9a$. The total structure factor and the partial
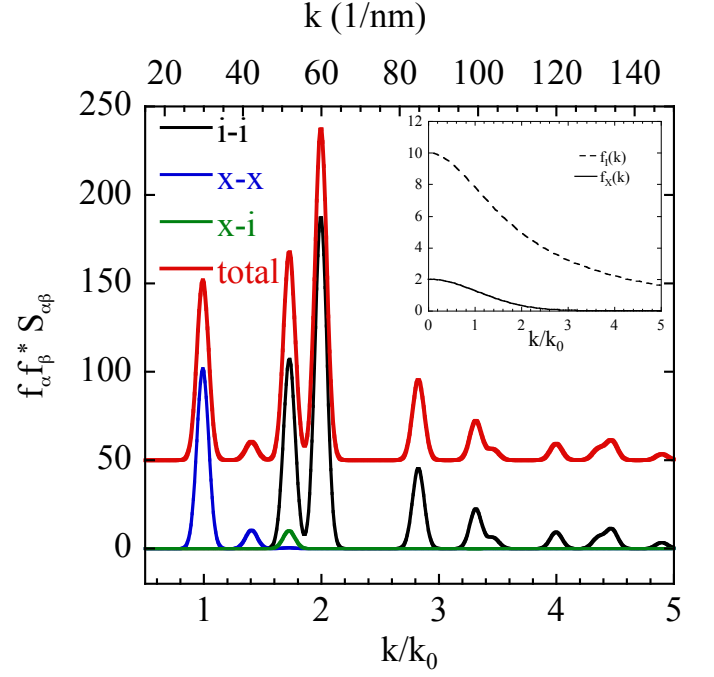

FIG. 1: Structure of Mg at ~ 500 GPa: Partial and total static structure factors for the fcc electride lattice. The inset shows the form factors for lattice ions (dashed) and interstitial electrons (solid).
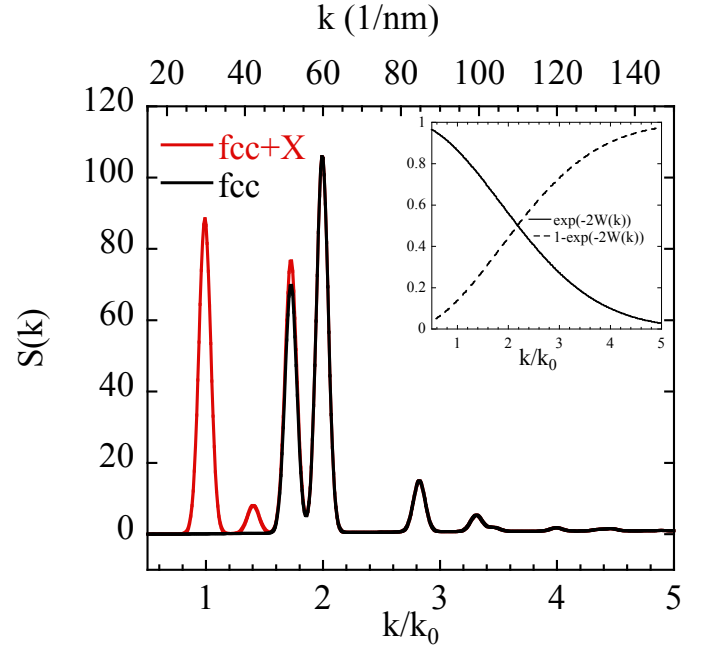

FIG. 2: Total elastic structure factor for the pure fcc lattice (black) and including interstitial electrons (red). The inset shows the Debye-Waller functions that describe the decay in Bragg intensity due to thermal lattice vibrations (solid line) and the amount of thermal diffuse scattering (dashed).

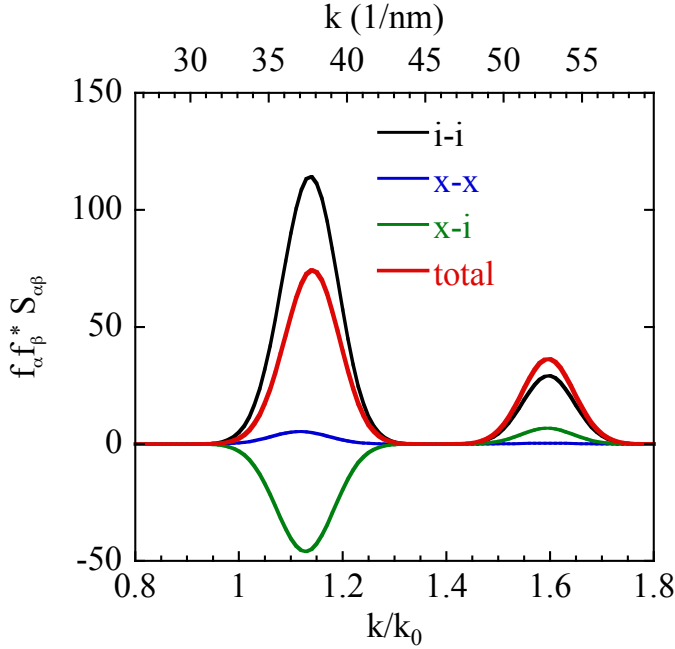structure factors are shown in Fig. 3. No additional re-

FIG. 3: Static structure factors for Mg at $800\,\mathrm{GPa}$.

FIG. 4: Scattering profiles for fcc and sh electride phases in Mg at ultrahigh pressures.

flections are observed in the total structure compared to the ion-ion structure. Instead, being of the same order as $S_{ii}(k)$, the interference term $S_{xi}(k)$ strongly affects the total signal. In the vicinity of the first Bragg peak ($k = k_0$), the interference term is negative, hence this peak is reduced in intensity by $\sim 30\%$. Conversely, the second peak is slightly enhanced through the interference term by $\sim 10\%$. This observation allows to identifiy the presence of intestitial electrons by comparing the peak intensities of the first two correlation peaks in an angle resolved x-ray scattering experiment. No absolute intensity measurement is required. Furthermore, the sh electride structure is greatly different from the lower pressure fcc electride structure as can be seen in Fig. 4. Due to higher compression, the position of the first (100) correlation peak is shifted to higher wavenumbers. Also, the coordination number is decreased from 12 to 8 and the number of ions per unit cell is reduced from 4 to 1 when going from fcc to sh phase, explaining the drop in overall intensity between both phases. Hence, observation of the location of the low k peaks and the overall scattering intensities will enables us to observe the phase transition between fcc and sh phase predicted at 756 GPa.

In conclusion, we have presented a model for the calculation of static structure factors for high pressure electride systems. Application of the model to predicted high pressure structures for Mg have shown that the existence of such phases is to be demonstrated unambigiously through angle resolved scattering of multi keV x-rays from ramp compressed targets, generated e.g. by a sequence of las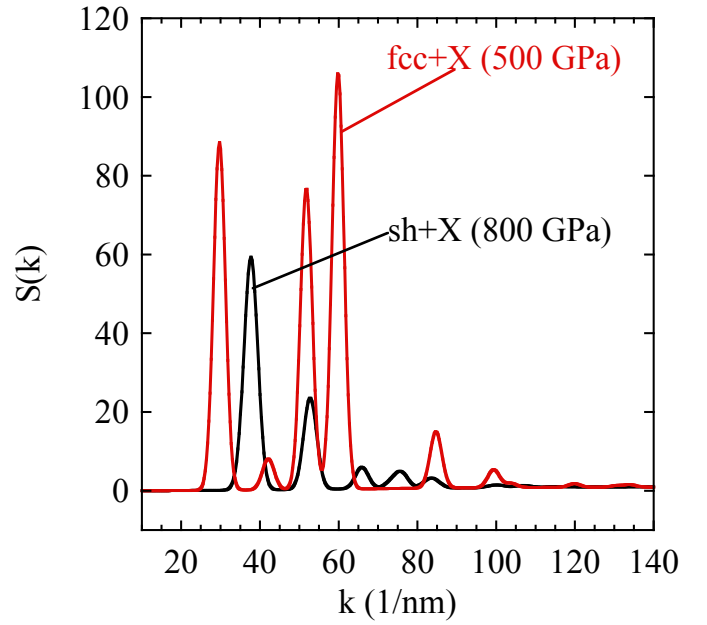er shocks. The additional correlation peaks in the fcc phase due to electron-electron correlations as well as the qualitative change in relative peak amplitudes in the sh phase due to electron-ion interference provide clearly detectable criteria that allow for a decisive experiment to verify the existence of high pressure electride phases in Mg and to show the structural phase transition between fcc and sh electride phase. The presented model can easily be applied to other materials, e.g. Li or Al to predict and to analyse x-ray scattering data from high pressure electrides. Having calculated the electron-electron structure factor, important quantities like transport coefficients, thermodynamic parameters (e.g. compressibility), and collective modes like phonons and plasmons can be predicted. This will be subject of a forthcoming publication.

[1] B. A. Remington, R. P. Drake, and D. D. Ryutov, Rev. Mod. Phys. **78**, 755 (2006), http://link.aps.org/doi/10.1103/RevModPhys.78.755
[2] R. W. Lee, S. J. Moon, H.-K. Chung, W. Rozmus, H. A. Baldis, G. Gregori, R. C. Cauble, O. L. Landen, J. S. Wark, A. Ng, S. J. Rose, C. L. Lewis, D. Riley, J.-C. Gauthier, and P. Audebert, J. Opt. Soc. Am. B **20**, 770 (Apr 2003), http://josab.osa.org/abstract.cfm?URI=josab-20-4-770

[3] S. P. Hau-Riege, A. Graf, T. Döppner, R. A. London, J. Krzywinski, C. Fortmann, S. H. Glenzer, M. Frank, K. Sokolowski-Tinten, M. Messerschmidt, C. Bostedt, S. Schorb, J. A. Bradley, A. Lutman, D. Rolles, A. Rudenko, and B. Rudek, Phys. Rev. Lett. **108**, 217402 (May 2012), http://link.aps.org/doi/10.1103/PhysRevLett.108.217402

[4] S. M. Vinko, O. Ciricosta, B. I. Cho, K. Engelhorn, H.-K. Chung, C. R. D. Brown, T. Burian, J. Chalupsky, R. W. Falcone, C. Graves, V. Hajkova, A. Higginbotham, L. Juha, J. Krzywinski, H. J. Lee, M. Messerschmidt, C. D. Murphy, Y. Ping, A. Scherz, W. Schlotter, S. Toleikis, J. J. Turner, L. Vysin, T. Wang, B. Wu, U. Zastrau, D. Zhu, R. W. Lee, P. A. Heimann, B. Nagler, and J. S. Wark, Nature **482**, 59 (2012)

[5] L. Young, E. P. Kanter, B. Krässig, Y. Li, A. M. March, S. T. Pratt, R. Santra, S. H. Southworth, N. Rohringer, L. F. DiMauro, G. Doumy, C. A. Roedig, N. Berrah, L. Fang, M. Hoener, P. H. Bucksbaum, J. P. Cryan, S. Ghimire, J. M. Glownia, D. A. Reis, J. D. Bozek, C. Bostedt, and M. Messerschmidt, Nature **466**, 56 (2010)

[6] R. R. Fäustlin, T. Bornath, T. Döppner, S. Düsterer, E. Förster, C. Fortmann, S. H. Glenzer, S. Göde, G. Gregori, R. Irsig, T. Laarmann, H. J. Lee, B. Li, K.-H. Meiwes-Broer, J. Mithen, B. Nagler, A. Przystawik, H. Redlin, R. Redmer, H. Reinholz, G. Röpke, F. Tavella, R. Thiele, J. Tiggesbäumker, S. Toleikis, I. Uschmann, S. M. Vinko, T. Whitcher, U. Zastrau, B. Ziaja, and T. Tschentscher, Phys. Rev. Lett. **104**, 125002 (2010)

[7] M. K. Matzen, M. A. Sweeney, R. G. Adams, J. R. Asay, J. E. Bailey, G. R. Bennett, D. E. Bliss, D. D. Bloomquist, T. A. Brunner, R. B. Campbell, G. A. Chandler, C. A. Coverdale, M. E. Cuneo, J.-P. Davis, C. Deeney, M. P. Desjarlais, G. L. Donovan, C. J. Garasi, T. A. Haill, C. A. Hall, D. L. Hanson, M. J. Hurst, B. Jones, M. D. Knudson, R. J. Leeper, R. W. Lemke, M. G. Mazarakis, D. H. McDaniel, T. A. Mehlhorn, T. J. Nash, C. L. Olson, J. L. Porter, P. K. Rambo, S. E. Rosenthal, G. A. Rochau, L. E. Ruggles, C. L. Ruiz, T. W. L. Sanford, J. F. Seamen, D. B. Sinars, S. A. Slutz, I. C. Smith, K. W. Struve, W. A. Stygar, R. A. Vesey, E. A. Weinbrecht, D. F. Wenger, and E. P. Yu, Physics of Plasmas **12**, 055503 (2005), http://link.aip.org/link/?PHP/12/055503/1

[8] J. D. Lindl, P. Amendt, R. L. Berger, S. G. Glendinning, S. H. Glenzer, S. W. Haan, R. L. Kauffman, O. L. Landen, and L. J. Suter, Phys. Plasmas **11**, 339 (2004)

[9] Y. B. Zel'Dovich and Y. P. Raizer, *Physics of shock waves and high-temperature hydrodynamic phenomena* (Dover Pubns, 2002) http://books.google.com/books?hl=en&lr=&id=zVf27TMNdToC&oi=fnd&pg=PR6&dq=Physics+of+shock-waves+and+high+temperature+hydrodynamic+phenomena&ots=C_liwOIa8Q&sig=hJxgU5rGruc85dGoxE1vx9G0kg8

[10] J. Hawreliak, J. Colvin, J. Eggert, D. Kalantar, H. Lorenzana, S. Pollaine, K. Rosolankova, B. Remington, J. Stlken, and J. Wark, Astrophysics and Space Science **307**, 285 (2007), ISSN 0004-640X, 10.1007/s10509-007-9385-z, http://dx.doi.org/10.1007/s10509-007-9385-z

[11] C. J. Pickard and R. J. Needs, Phys. Rev. Lett. **97**, 045504 (2006), http://link.aps.org/doi/10.1103/PhysRevLett.97.045504

[12] M. Marqués, M. Santoro, C. Guillaume, F. Gorelli, J. Contreras-García, R. Howie, A. Goncharov, and E. Gregoryanz, Physical Review B **83**, 1 (2011), ISSN 1098-0121, http://link.aps.org/doi/10.1103/PhysRevB.83.184106

[13] M. Marqués, G. Ackland, L. Lundegaard, G. Stinton, R. Nelmes, M. McMahon, and J. Contreras-García, Phys. Rev. Lett. **103**, 9 (2009), ISSN 0031-9007, http://link.aps.org/doi/10.1103/PhysRevLett.103.115501

[14] P. Li, G. Gao, Y. Wang, and Y. Ma, The Journal of Physical Chemistry C **114**, 21745 (2010), http://pubs.acs.org/doi/abs/10.1021/jp108136r

[15] C. J. Pickard and R. J. Needs, Nat. Mater. **9**, 624 (2010)

[16] J. B. Neaton and N. W. Ashcroft, Nature **400**, 141 (1999), ISSN 0028-0836

[17] Y. Ma, M. Eremets, A. R. Oganov, Y. Xie, I. Trojan, S. Medvedev, A. O. Lyakhov, M. Valle, and V. Prakapenka, Nature **458**, 182 (2009), ISSN 00280836, http://dx.doi.org/10.1038/nature07786

[18] H. Jones, Proceedings of the Royal Society of London. Series A - Mathematical and Physical Sciences **147**, 396 (1934), http://rspa.royalsocietypublishing.org/content/147/861/396.full.pdf+html http://rspa.royalsocietypublishing.org/content/147/861/396.short

[19] J. L. Dye, Science (New York, N.Y.) **247**, 663 (1990), ISSN 0036-8075, http://www.sciencemag.org/content/247/4943/663.abstracthttp://www.sciencemag.org/content/247/4943/663.full.pdfhttp://www.ncbi.nlm.nih.gov/pubmed/17771882

[20] S. Matsuishi, Y. Toda, M. Miyakawa, K. Hayashi, T. Kamiya, M. Hirano, I. Tanaka, and H. Hosono, Science (New York, N.Y.) **301**, 626 (2003), ISSN 1095-9203, http://www.ncbi.nlm.nih.gov/pubmed/12893938

[21] J. L. Dye, Science **301**, 607 (February 2003), ISSN 0036-8075, http://www.ncbi.nlm.nih.gov/pubmed/12893933http://www.sciencemag.org/content/301/5633/607.full.abstracthttp://www.sciencemag.org/content/301/5633/607.full.full.pdf

[22] H.-k. Mao and R. J. Hemley, Rev. Mod. Phys. **66**, 671 (April 1994), http://link.aps.org/doi/10.1103/RevModPhys.66.671

[23] S. H. Glenzer and R. Redmer, Rev. Mod. Phys. **81**, 1625 (2009), http://adsabs.harvard.edu/abs/2009RvMP...81.1625G

[24] D. A. Baiko, A. D. Kaminker, A. Y. Potekhin, and D. G. Yakovlev, Phys. Rev. Lett. **81**, 5556 (1998)

[25] C. Kittel, *Quantum theory of solids* (Wiley, New York, 1963)

[26] A. D. Becke and K. E. Edgecombe, The Journal of Chemical Physics **92**, 5397 (1990), http://link.aip.org/link/?JCP/92/5397/1

[27]

[28] 08(1)